Annu. Rev. Earth Planet. Sci. 1991. 19:423–55

EXPERIMENTAL DETERMINATION OF BED-FORM STABILITY

John B. Southard

Department of Earth, Atmospheric, and Planetary Sciences,
Massachusetts Institute of Technology, Cambridge, Massachusetts 02139

KEY WORDS: bed configurations, bed forms, combined flows, oscillatory flows, unidirectional flows

INTRODUCTION

A striking characteristic of the transport of granular sediment over a bed of the same material by a turbulent flow of fluid is that over a wide range of conditions the bed is molded into topographic features—bed forms—on a scale orders of magnitude larger than the grains. Little ripples at one's feet at the seashore, or on a dry river bed, or in the desert; gigantic dunes in the desert and (even more common, but not apparent to the casual observer) in large rivers and the shallow ocean—all of these are examples of bed forms. Generations of scientists and engineers have marveled at the rich and confusing variety of these features.

The overall bed geometry that exists at a given time in response to the flow (the *bed configuration*) is composed of individual topographic elements (*bed forms*). The aggregate or ensemble of like bed configurations that can be produced by a given mean flow over a given sediment bed is the *bed state*: The bed configuration changes in details from time to time, but the bed state represents the infinity of configurations possible under the given conditions of flow and sediment. The term *bed phase* can be used for recognizably or qualitatively different kinds of bed states that are produced over some range of flow and sediment conditions and are closely related in geometry and dynamics. Finally, the term *bedform* (one word) is widely used, indiscriminately, for all four aspects of the bed geometry.

Even apart from their intrinsic interest, bed forms are important in both

0084–6597/91/0515–0423$02.00

geology and engineering. Large subaqueous bed forms many meters high can be obstacles to navigation, and their movement can be a threat to submarine structures. The rugged topography of bed forms in rivers and tidal channels causes flow separation at the crests and therefore large values of form drag; bed forms are thus the most important determinant of resistance to channel flow, and hydraulic engineers have expended much effort on the development of depth-discharge predictors based on the hydraulic relationships of the bed states (Vanoni 1975, pp. 114–52). The bed state is also closely bound up with the sediment transport rate in unidirectional flows, in that the downcurrent movement of the bed forms largely involves recycling of bed load within bed forms. Sedimentologists have given attention to bed forms mostly because of their role in generating stratification in sedimentary deposits—one of the most useful tools available for interpreting ancient sedimentary environments.

This paper systematically reviews what is known experimentally about the ranges of existence of the various bed phases in unidirectional, oscillatory, and combined flows by using suitable dimensionless variables in a graphical framework appropriately simplified for each kind of flow. Parts of this review are along the lines of earlier papers by the writer (Harms et al 1982, Middleton & Southard 1984, Southard & Boguchwal 1990). There have been many other reviews of bed configurations in unidirectional and oscillatory flows from a variety of standpoints (e.g. Komar 1974, Clifton 1976, Harms 1979, Nielsen 1981, Allen 1982, Engelund & Fredsøe 1982, Clifton & Dingler 1984, Vongvisessomjai 1984, Ashley 1990).

This review limits itself to experiments on bed configurations in laboratory channels. There have been a great many studies of bed configurations in natural flow environments, mostly in flows much deeper than those in the laboratory. For reviews of such studies, see Allen (1982, Vol. 1) and Ashley (1990). There is a continuing need for integration of the laboratory work with observations on fluvial and marine bed configurations (cf Rubin & McCulloch 1980). The problem with using field studies to define bed-phase stability fields except in a general way is that steady flow leading to an equilibrium bed state is the exception in the natural environment. The virtue of flume work, despite the largely too shallow flow depths, is that it permits systematic study of the stability relationships, which in turn serve as a guide to the usually less steady natural flows. The present review is offered in that spirit.

The earliest important experimental work on bed configurations was by Sorby (1859, 1908) many decades ago. The first large unidirectional-flow experimental program was by Gilbert (1914); even today, Gilbert's work has not lost its value. The "modern era" of experiments on bed configurations in unidirectional flows can be said to have begun with the

extensive work by Simons and coworkers (Simons et al 1961, Simons & Richardson 1963, 1966, Guy et al 1966). Since the 1950s, there have been many other sets of experiments; prominent among many others are those of Vanoni and coworkers (Vanoni & Brooks 1957, Kennedy 1961), Chabert & Chauvin (1963; see also Laboratoire National d'Hydraulique 1961), Stein (1965), Williams (1967, 1970), Pratt (1971), Willis et al (1972), Nordin (1976), and Costello & Southard (1981).

Systematic modern experiments on oscillatory-flow bed configurations commenced with the work of Bagnold (1946). Subsequent studies include those of Kennedy & Falcón (1965), Carstens & Neilson (1967), Carstens et al (1969), Mogridge & Kamphuis (1972), Lofquist (1978), and Southard et al (1990), among others. Observations on combined-flow bed configurations, exemplified by the work of Inman & Bowen (1963), Harms (1969), Brevik & Aas (1980), and Arnott & Southard (1990), have so far been extremely limited.

THE NATURE OF BED CONFIGURATIONS

Distinctive bed forms are most common in sands, but they are produced in silts and gravels as well. Of greatest interest to geologists are bed forms produced by flows of air or water over mineral sediments, but a far wider range can be produced by flows of Newtonian fluids with other densities and viscosities over sediments less dense or more dense than the common mineral sediments. This review concentrates on bed configurations developed by flows of water over quartz-density sediments.

Bed configurations are molded not only by purely unidirectional or purely oscillatory flows but also by all combinations of the two. In natural flows each of these components tends to vary in speed and direction with time, and the oscillatory component itself commonly has a discrete or continuous range of periods and directions. This enormous range of combined flows, together with the complex dynamics of the response of the bed, makes for extremely varied geometry of the resulting bed forms. For the most part, only the simplest end members of this range of flows have been used in laboratory studies of bed configurations.

The variety in geometry as well as in scale of bed forms is striking. Scales span a range of five orders of magnitude, from a few centimeters to over 1000 m in spacing. Bed forms tend to be flow transverse, although flow-parallel forms are produced by unidirectional flows under certain conditions, and forms with no strongly preferred orientation are produced in some oscillatory flows. Most bed forms are irregular in detail but tend to show a more or less strong element of regularity in their overall arrangement; some are so regular as to be almost perfectly cylindrical or

two dimensional. Transverse bed forms in flows with a unidirectional component move upstream or downstream at a speed much slower than the flow speed by means of erosion of sediment on one flank and deposition on the other. Most bed forms are at least crudely wave shaped and are often likened to waves; in fact, they are not waves in the dynamic sense, although they can be viewed as kinematic waves (Langbein & Leopold 1968, Costello & Southard 1981, Song 1983).

If queried, a scientist from a sediment-free planet would probably surmise that the natural mode of grain transport by a flowing fluid would be over a planar bed. In certain ranges of flow, a planar transport surface is indeed the stable bed configuration. (Such a plane bed is a bed configuration with no bed forms.) Only in laminar flows, however, is this invariably so. In turbulent flows, plane-bed transport is the stable configuration under certain conditions, but bed forms are the dominant transport surface in both oscillatory and unidirectional flows. In unidirectional flows, over a wide range of flows and sediment sizes a planar transport surface is unstable to small perturbations, and otherwise insignificant geometrical irregularities, either preexisting or flow generated, are amplified to become bed forms. As the flow molds the bed by erosion and deposition, the bed geometry thus generated changes the structure of the flow itself in fundamental ways that are difficult to parameterize. There is thus a strong interaction or feedback between the bed and the flow, and this essential element of complexity has hindered the development of theory. For recent work on the theory of flow-transverse bed forms, see Richards (1980), Hayashi & Onishi (1983), Sumer & Bakioglu (1984), and Kobayashi & Madsen (1985). In contrast, flow-parallel bed forms seem to be produced either by flow-parallel helical secondary flow cells superimposed on the main flow or by alternating sediment movement by two flows at some angle to one another (Rubin & Hunter 1987). In oscillatory flows, repetitive bed forms seem, for the most part, to be engendered by a regular pattern of convergent and divergent flow at the bed that scales with the orbital diameter of the oscillation (Sleath 1975, 1976, Kaneko & Honji 1979a,b, Longuet-Higgins 1981).

The status of observations on bed configurations leaves much to be desired. It is easy to observe bed configurations in steady unidirectional and bidirectional symmetrically oscillatory flows in laboratory channels and tanks, and the major outlines are by now fairly well known. But there is much room for further laboratory work: The usually small width-to-depth ratios of tanks and flumes tend to inhibit full development of the three-dimensional aspects of the bed geometry (which are crucial in determining the geometry of the resultant sedimentary structures), and virtually no work has been done with multidirectional oscillatory flows, with or

without a unidirectional component. And even the largest laboratory experiments are restricted to flow depths at the lower end of the range of natural flow depths. In nature, on the other hand, observations of bed configurations are limited by practical and technical difficulties, and the generating flows are usually more complex.

If the flow changes with time, the bed configuration adjusts in response. In natural flows, equilibrium between the bed and the flow is the exception rather than the rule; usually the bed configuration lags behind the change in the flow. This lag effect can range from slight to gross. Such disequilibrium is a major element of complexity that makes relationships among bed phases much more difficult to decipher, but its effects are important in natural flow environments and therefore significant for interpretation of sedimentary structures. Allen (1974, 1976a,b, and other papers) and Fredsøe (1979, 1981) have developed theoretical approaches to disequilibrium effects, but the only experimental work seems to have been by Simons & Richardson (1962a,b) and Gee (1975).

CONCEPTUAL FRAMEWORK

The strategy here is to list the most important variables associated with the fluid, the sediment, and the flow that define the bed state, and then to develop an appropriate corresponding set of dimensionless variables that most effectively characterizes the bed state. One can then imagine graphing, with these dimensionless variables along the axes, the positions of bed states produced in laboratory tanks and channels in order to identify the fields of existence or stability of the various bed phases. The resulting diagram, which is analogous to the thermodynamic phase diagrams used to represent the stability relations of mineral phases, is filled with stability regions for the various bed phases; boundaries between these stability regions are either well-defined surfaces or transitional zones. Bed-phase diagrams of this kind, based upon certain subsets of axis variables corresponding to certain subranges of conditions in which one or more dimensionless variables can be safely neglected, systematize and unify disparate data on bed states over a wide variety of flows and sediments.

To be sufficiently general, such a graph must have a minimum of more than three dimensions no matter how it is arranged, but three-dimensional "sections" through it are suitable for representing bed phases in steady unidirectional flows or symmetrical bidirectional oscillatory flows. With the data now available, such graphs can be drawn only for equilibrium bed states in quasi-steady flows, but these serve as a reference for interpreting the more complicated disequilibrium bed states that are so important in natural flows.

Identification of the variables is not straightforward. Even for equilibrium bed states in quasi-steady flows the number is actually infinite, for two reasons: (*a*) Oscillatory flows can have a continuous range of periods and directions, and (*b*) an infinite number of variables are needed to describe a general joint probability distribution of sediment grain size and shape. Consideration is limited here to flows with a single oscillatory component because no laboratory data are yet available for more general oscillatory flows. Also, it is assumed that in any given case the sediment is of one density and grain shape and has an approximately log-normally distributed size, so that it can be characterized fairly well by the mean or median size D, some measure of sorting like the standard deviation σ of the size distribution, and the density ρ_s.[1] In most cases of relevance to natural environments, the sediment is indeed equant, fairly well sorted, and of about quartz density. Two variables, density ρ and viscosity μ, are needed for the fluid (neglecting elasticity and surface tension). The submerged weight per unit volume of the sediment, γ', must be included, in addition to the density of the sediment, to take account of weight as well as inertia of the particles.

Five variables are needed to describe the state of the flow. One is the angle θ between the unidirectional- and oscillatory-flow directions. The oscillatory component can be described by two of the following three variables: oscillation period T, maximum orbital speed U_o, and orbital diameter d_o (the maximum excursion distance of water particles outside the oscillatory boundary layer). The unidirectional component can be described by the flow depth d (largely irrelevant for atmospheric flows) and any one of several flow-strength variables: discharge per unit width of flow q, mean flow velocity U_u, mean boundary shear stress τ_o, or flow power $P = \tau_o U_u$. The three considerations here are, (*a*) Which variables are truly independent, in the sense that they are imposed upon the system and are unaffected by its operation? (*b*) Which variables characterize the bed state, in the sense that their specification unambiguously identifies the bed state, whether or not they are independent? (*c*) Which variables govern the bed state, in the sense that they are dynamically most directly responsible for the bed state, whether or not they are independent?

The main goal of this review is to show unambiguously the hydraulic relationships among bed phases, ideally as a one-to-one correlation between bed states and combinations of variables, so that stability fields for the bed phases fill the phase diagram exhaustively and do not overlap. In this respect, U_u (or q) is the most appropriate unidirectional flow-

[1] A complete listing of the symbols used in this paper can be found following the *Literature Cited* section.

strength variable because, for a given fluid, each combination of U_u and d in steady uniform flow corresponds to exactly one average state of the flow, in terms of velocity structure and boundary forces. This is not the case, however, with τ_o or P; with these variables, there is an element of ambiguity in that for certain values of τ_o or P more than one bed state at a given flow depth is possible (Brooks 1958, Kennedy & Brooks 1963). This has to do with the great decrease in form resistance in the transition from ripples to plane bed with increasing U_u or q at constant d. Independence need not be a criterion in choice of variables to describe the bed state, because a given set of variables can equally well describe the bed state whether any given variable in the set is dependent or independent: The bed state is a function of the nature of the flow but not of how the flow is arranged or established.

It might seem that τ_o is more logical than U_u for characterizing the effect of the flow on the bed because the sediment is caused to be transported by the force exerted by the flow on the bed. But on beds with rugged flow-transverse bed forms, only a small part of τ_o represents the boundary friction responsible for grain transport, the rest being form drag on the main roughness elements. So, in one important sense, τ_o is no less a surrogate variable than U_u.

The final number of characterizing variables is thus 11:

$$\text{bed state} = f(U_u, U_o, d, T, \theta, D, \rho, \mu, \rho_s, \gamma', \sigma).$$

Dimensional analysis should thus yield an equivalent set of 8 dimensionless variables (Buckingham 1914; cf Middleton & Southard 1984). Many such sets are possible; the criterion for a choice here is sedimentological usefulness rather than dynamical significance. In the view that U_u, U_o, T, d, and D are of greatest interest to geologists, these five are segregated into separate dimensionless variables—respectively, dimensionless unidirectional flow speed $U_u^\circ = U_u(\rho^2/\mu\gamma')^{1/3}$, dimensionless oscillatory flow speed $U_o^\circ = U_o(\rho^2/\mu\gamma')^{1/3}$, dimensionless oscillation period $T^\circ = (\gamma'^2/\rho\mu)^{1/3}$, dimensionless flow depth $d^\circ = d(\rho\gamma'/\mu^2)^{1/3}$, and dimensionless sediment size $D^\circ = D(\rho\gamma'/\mu^2)^{1/3}$. The remaining three dimensionless variables are θ, σ/D, and ρ_s/ρ.

Even for a given combination of fluid and sediment density and neglecting σ/D as being of secondary importance, one is left with an impossible five-dimensional graph for each value of θ. For further simplification it is assumed that, for purely unidirectional flows, θ, U_o°, and T° are irrelevant, leaving a workable three-dimensional graph of d°, U_u°, and D° (here called the depth-speed-size diagram) for each ρ_s/ρ. Two such graphs, for quartz-density sediment in water and in air, are geologically most relevant; only the graph for water is considered below. It is similarly assumed that, for

purely oscillatory flows, U_u and d are irrelevant, leaving a workable three-dimensional graph of T^o, U_o^o, and D^o (here called the period-speed-size diagram) for each ρ_s/ρ; only that for quartz-density sediment in water is of substantial geological interest. For combined flows one is still left with a four-dimensional graph for each ρ_s/ρ, although presumably T^o is less important than d^o for current-dominated flow, and d^o is less important than T^o for oscillation-dominated flow.

THE EFFECTS OF FLUID TEMPERATURE

Over a range of water temperatures from 0 to 30°C at the Earth's surface, ρ and γ' are nearly constant but μ decreases by a factor of about 0.45. A bed-phase diagram using the dimensional variables U_u, U_o, T, d, and D rather than the corresponding dimensionless variables would therefore show scatter if the data covered a range of water temperatures.

In the bed-phase graphs below, the dimensionless variables U_u^o, U_o^o, T^o, d^o, and D^o have been converted to values U_{u10}, U_{o10}, d_{10}, T_{10}, and D_{10} corresponding to an arbitrary reference temperature of 10°C; in this way the dimensionless nature of the graphs is preserved while still giving a concrete idea of flow and sediment conditions. This is easily done by formulating each dimensionless variable both from the given conditions and from the 10°C conditions, setting the two equal, and solving for the 10°C value (Southard & Boguchwal 1990). Neglecting the slight variation of ρ and γ' with temperature, the result for D_{10} is $D(\mu_{10}/\mu)^{2/3}$, and d_{10} is of the same form; the result for U_{u10} is $U(\mu_{10}/\mu)^{1/3}$, and U_{o10} and T_{10} are of the same form. (Here μ_{10} is the fluid viscosity standardized to 10°C water temperature.)

The eight dimensionless variables in the previous section are also scale-modeling parameters. Any number of geometrically similar flows are possible in which U_u, U_o, T, d, D, ρ, μ, ρ_s, γ', σ, and θ are adjusted so that each dimensionless variable has the same value in all of the flows; each such flow is a dynamic scale model of all the others, in the sense that all forces and motions are in the same proportions among the flows. This is an example of Reynolds-Froude scale modeling. Similitude conditions for the modeling of one flow by another are found by setting each of the dimensionless variables equal in modeled flow and modeling flow and solving for the ratios of U_u, U_o, d, T, and D in the modeling flow and the modeled flow in terms of the ratios of the various system properties ρ, μ, ρ_s, and γ' (cf Southard et al 1980). The result for the length scale ratios d_r and D_r is that $d_r = D_r = (\mu_r/\rho_r)^{2/3}$, and the result for the velocity ratios and the period ratio is that $U_{ur} = U_{or} = T_r = (\mu_r/\rho_r)^{1/3}$, where the subscript "r"

denotes the ratio of d, U, or D between the modeling flow and the modeled flow.

Given two dynamically similar flows, the sense of the difference in scale for a difference in water temperature is thus that the flow depth, sediment size, bed-form size, oscillatory and unidirectional velocity components, bed-form velocity, and oscillation period in the cold-water flow are all larger than in the hot-water flow. The length variables in a flow at 0°C are greater by a factor of 1.7, and the velocity variables and the period are greater by a factor of 1.3 than in a flow at 30°C.

CLASSIFICATION OF BED STATES

The classification of bed states in unidirectional and oscillatory flows into bed phases has long been debated but is hampered by a scarcity of data from the more general combined flows, of which purely unidirectional or oscillatory flows are merely end-member cases. Bed states in unidirectional sediment-moving water flows are conventionally classified into ripples, dunes, plane beds (in two different regimes), and antidunes.

Ripples (Figure 1) are small-scale ridge-and-trough bed forms oriented dominantly transverse to flow. Their downcurrent surfaces have slopes usually at or near the angle of repose of the sediment (of the order of 30°), and their upcurrent slopes are usually much gentler. Spacings are usually 0.1–0.2 m, and heights are usually no more than a few centimeters. When fully developed, they show substantial irregularity in geometry: Crests and troughs tend to be sinuous and variable in height, and when traced laterally individual ripple crests terminate by merging with another ripple crest or disappearing into a trough. Ripples move in the downcurrent direction at speeds orders of magnitude less than the flow velocity by means of erosion of sediment from the upstream surface and deposition on the downstream surface.

There is a break in size between current ripples, on the one hand, and the various large-scale flow-transverse bed forms variously termed dunes, megaripples, and sand waves, on the other. Following Ashley (1990), we lump all such large-scale bed forms under the term dunes. These features are much like ripples in geometry and movement. Their spacing ranges upward from somewhat less than half a meter to thousands of meters. At relatively low flow strengths dunes tend to be regular and straight crested (two-dimensional dunes; Figure 2), whereas at relatively high flow strengths they tend to be sinuous and discontinuous, with strong variability in crest and trough heights (three-dimensional dunes; Figure 3).

Antidunes (Figure 4) are upstream-moving undulations of the sediment

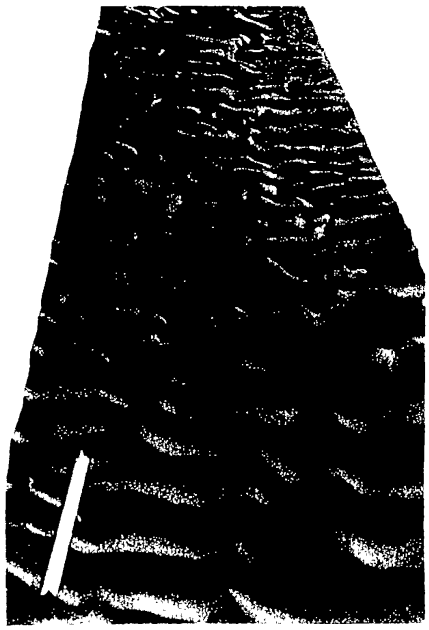

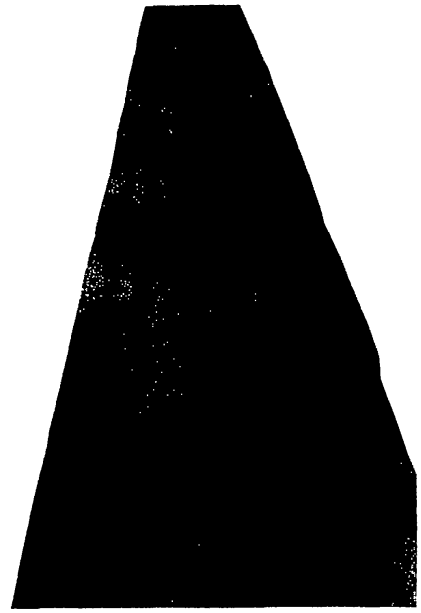

Figure 1 (*Left*) Ripples in unidirectional flow. Flow is from top to bottom; channel is 0.92 m wide. Black areas are water puddles. $U_{u10} = 0.32$ m/s; $d_{10} = 0.22$ m, $D_{10} = 0.83$ mm.
Figure 2 (*Right*) Two-dimensional dunes in unidirectional flow. Flow is from top to bottom; channel is 0.92 m wide. Black areas are water puddles. $U_{u10} = 0.47$ m/s, $d_{10} = 0.21$ m, $D_{10} = 0.89$ mm.

bed in phase with water-surface waves, which are stationary or slowly upstream moving. Trains of antidunes tend to grow to unstable steepness, break, and then slowly reform. Antidunes range from short crested to long crested.

In oscillatory flows, the very regular straight-crested ripples that form at short to moderate periods and over a wide range of velocities have always been called oscillation ripples or wave ripples. Most of these can be classified as vortex ripples (Bagnold 1946), in reference to the characteristic mode of flow and sediment movement. Most, but not all, vortex ripples can also be classified as orbital ripples (Clifton 1976), in that their spacing scales with the orbital diameter of the oscillation, in contrast to suborbital ripples and anorbital ripples, whose spacing scales less strongly (or not at all) with orbital diameter. Also, Clifton et al (1971) have described small ripples, called reversing-crest ripples, that change their sense of asymmetry and direction of movement significantly over each oscillation. With increasing U_o and T, vortex ripples become three dimensional rather than two dimensional (Carstens & Neilson 1967, Carstens et al 1969, Southard et al 1990). In the synthesis below, the problem of terminology for oscillatory-flow bed states is streamlined by using two genetic terms—oscillatory-current ripples and reversing-current ripples (Southard et al 1990).

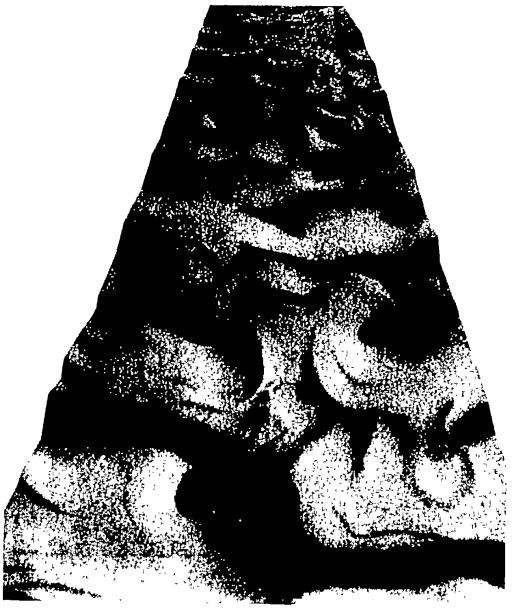

Figure 3 (*Left*) Three-dimensional dunes in unidirectional flow. Flow is from top to bottom; channel is 0.92 m wide. Black areas are water puddles. $U_{u10} = 0.60$ m/s, $d_{10} = 0.20$ m, $D_{10} = 0/.95$ mm.

Figure 4 (*Right*) Water-surface manifestation of antidunes in unidirectional flow. Flow is from left to right. Largest pebbles are about 3 cm.

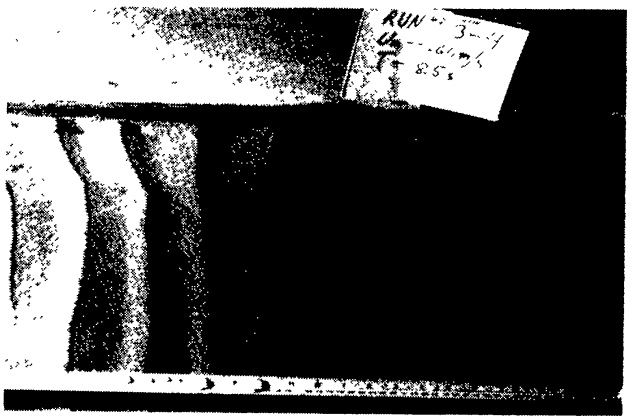

Figure 5 (*Left*) Two-dimensional oscillatory-current ripples. The scale, parallel to the oscillation direction, is 0.60 m long. $U_{o10} = 0.18$ m/s, $T_{10} = 9.3$ s, $D_{10} = 0.11$ mm.

Figure 6 (*Right*) Three-dimensional oscillatory-current ripples. The scale, parallel to the oscillation direction, is 0.56 m long. $U_{o10} = 0.35$ m/s, $T_{10} = 9.6$ s, $D_{10} = 0.11$ mm.

Oscillatory-current ripples are dependent upon the patterns of flow and sediment movement specific to the existence of the oscillation itself. These are the vortex ripples or orbital ripples mentioned above; they range from a few centimeters to a few meters in spacing, and their shape ranges from strictly two dimensional (Figure 5) to strongly three dimensional (Figure 6), depending upon D, U_o, and T. Reversing-current ripples are dependent only upon the existence of the current, in one direction or the other, during the oscillation. They are always small: Typical spacings are several centimeters, about the same as the spacings of unidirectional-flow ripples in their early stages of development, to which they are related in dynamics.

Combined-flow bed states are less easy to classify. The various ripples in purely oscillatory flows must somehow pass over into the ripples and dunes in purely unidirectional flows. These relationships are discussed further in a later section on combined-flow bed states.

BED CONFIGURATIONS IN UNIDIRECTIONAL FLOWS

General

Flume studies on sediment movement by unidirectional flows have concentrated mostly on either sediment transport rates or the geometry and hydraulic relationships of the bed configurations. Results on transport rates have been summarized in greatest detail by Brownlie (1981). Allen (1982) and Southard & Boguchwal (1990) have provided the most recent and most detailed syntheses of flume results on bed configurations. The following review is based mainly on the discussion by Southard & Boguchwal (1990).

Laboratory experiments on bed configurations are mostly made in rectangular open channels ("flumes") in which the water is almost always recirculated and the sediment is usually but not always recirculated. A thick layer of sediment is placed in the channel, and a flow with a certain depth and velocity is passed over it until the bed configuration has come into equilibrium with the flow. The time for attainment of equilibrium ranges from less than 1 hr to many hours or even tens of hours. Flow depth and energy slope are established for a given water discharge in various ways, but the manner in which they are established is irrelevant to the reproducibility of the ultimate bed state. With few exceptions, flow depths have been less than 1 m, and ratios of channel width to flow depth have generally not been large enough for fully representative development of the plan geometry of dunes. Few studies have been made with sediment finer than the finest sand sizes or coarser than about 10 mm.

Hundreds of flume runs have been made specifically to look at bed configurations, and a large number of transport-rate runs have reported the bed configuration in some detail as well. With the present coverage of data the general outlines of the hydraulic relationships among the various bed phases are fairly clear, but there are still many points of uncertainty in detail, especially because of the complexity of relationships at certain phase boundaries. A great many more runs in large flumes would be needed to sharpen our understanding of relationships significantly, but this is unlikely to occur.

Depth-Speed-Size Diagram

Southard & Boguchwal (1990) considered data from 39 flume studies that report water temperature and equilibrium bed state as well as d, U_u, and D. The classic work of Gilbert (1914) was omitted because temperature was not reported, and several otherwise eligible studies were not used because the bed configuration was not adequately described. Runs in which equilibrium was not attained or for which the width-to-depth ratio was less than about 3 were omitted. In all, 1950 runs were used. Series of d_{10}-U_{u10} sections and U_{u10}-D_{10} sections through the d_{10}-U_{u10}-D_{10} graph were drawn by dividing the ranges of d_{10} and D_{10} into narrow intervals, projecting available data onto the midplanes of those intervals, and drawing boundaries between bed-phase fields. Relationships among bed phases are discussed here with reference to three d_{10}-U_{u10} sections (Figure 7) and one U_{u10}-D_{10} section (Figure 8), chosen as generally showing relationships most clearly and having the largest number of data points.

The d_{10}-U_{u10} graph for 0.10–0.14 mm sand (Figure 7*A*) shows fields only for ripples, upper-regime plane beds, and antidunes. All of the boundaries here and in the other two d_{10}-U_{u10} sections in Figure 7 slope upward to the right. The ripple-plane boundary does so because the deeper the flow, the greater the velocity needed for a given bed shear stress; the plane-antidune boundary does so because it is closely associated with the condition for mean-flow Froude number $\mathrm{Fr} = U_u/(gD)^{1/2} = 1$, near which surface waves interact unstably with the bed to produce antidunes. The latter boundary is shown to truncate the former because (though data are scanty) as the Froude number approaches unity, antidunes develop no matter what the preexisting configuration. This relation holds true also, and more clearly, for coarser sediments (Figures 7*B*,*C*).

In Figure 7*A* (and in Figure 7*B*, for medium sands, as well) there are two kinds of boundary between movement and no movement. To the right is the Miller et al (1977) modification of the Shields curve for incipient movement on a plane bed, transformed into this d_{10}-U_{u10} graph. To the left is the ripple-maintenance boundary, which defines the minimum velocity

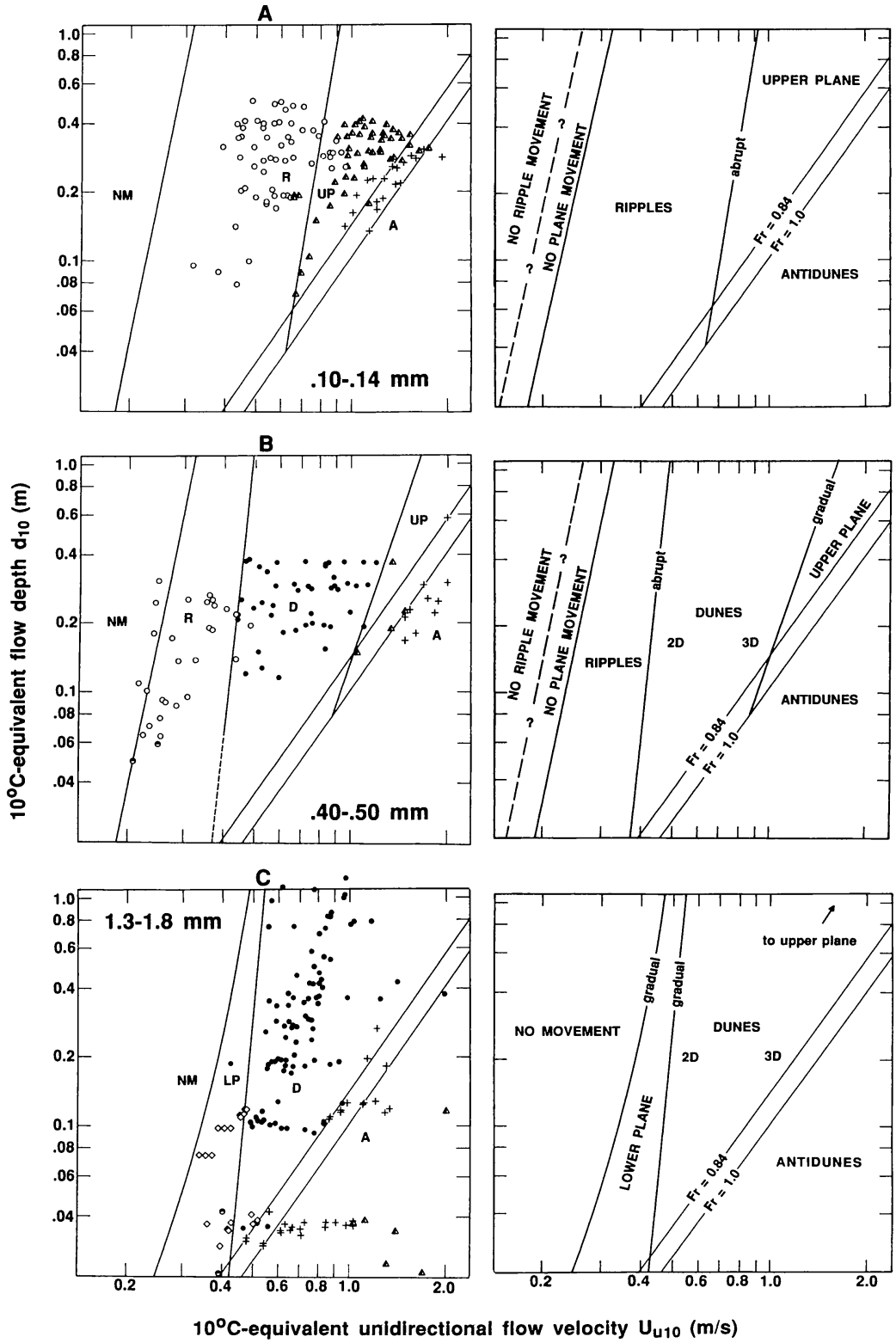

needed to maintain preexisting ripples at equilibrium. The ripple-maintenance boundary is not well constrained by data [and so is shown only in the cartoon (right frame)], but it clearly lies at lower flow velocities than the plane-bed threshold curve (cf Costello & Southard 1981).

The d_{10}-U_{u10} graph for 0.40–0.50 mm sand (Figure 7*B*) shows an additional field for dunes between those for ripples and plane beds, with its high-velocity boundary clearly sloping less steeply than its low-velocity boundary. For d_{10} less than about 0.05 m it is difficult to differentiate between ripples and dunes because dunes become severely limited in size by the shallow flow depth. The appearance and expansion of the dune field with increasing sediment size push the lower termination of the plane-bed field to greater d_{10} and U_{u10}, nearly out of the range of most flume work. The antidune field truncates not only the ripple field, as with finer sands, but the dune field as well.

In the d_{10}-U_{u10} graph for 1.30–1.80 mm sand (Figure 7*C*), a lower-regime plane bed replaces ripples at low flow velocities. The upper-regime plane bed is still present in the upper right, but few flume data are available. Upper-regime plane beds succeed antidunes with increasing U_{u10} and decreasing d_{10} in the lower right; apparently the bed becomes planar once again as the Froude number becomes sufficiently greater than unity. The boundary between no movement and lower plane beds is shown as the Miller et al (1977) modification of the Shields curve, with which the data are fairly consistent; discrepancies are to be expected because of the wide range of bed shear stresses for which there is weak bed-load movement. Sections for even greater D_{10} are qualitatively similar to that in Figure 7*C*.

In the U_{u10}-D_{10} graph for flow depths of 0.25–0.40 m (Figure 8), ripples are stable for D_{10} finer than about 0.8 mm. The range of U_{u10} for ripples narrows with increasing D_{10} to terminate against the fields for plane beds with or without movement. Relationships in this region are difficult to study because in these sand sizes and flow speeds it takes a long time for the bed to attain equilibrium. In medium sands ripples give way abruptly

Figure 7 Relationships of bed-phase stability fields in plots of d_{10} vs U_{u10} for three ranges of sediment size D_{10} in flumes. (*A*) 0.10–0.14 mm; (*B*) 0.40–0.50 mm; (*C*) 1.3–1.8 mm. For data sources, see Southard & Boguchwal (1990). The *left-hand* graphs show the data, and the *right-hand* graphs are schematic. Symbols: *open circles*, ripples; *solid circles*, dunes; *half-open circles*, undifferentiated ripples/dunes; *open diamonds*, lower-regime plane beds; *half-open triangles*, upper-regime plane beds; *plus signs*, antidunes. Abbreviations: NM, no movement on plane bed; R, ripples; D, dunes; LP, lower-regime plane beds; UP, upper-regime plane beds; A, antidunes. Modified slightly from Southard & Boguchwal (1990); reproduced with permission of SEPM (Society for Sedimentary Geology).

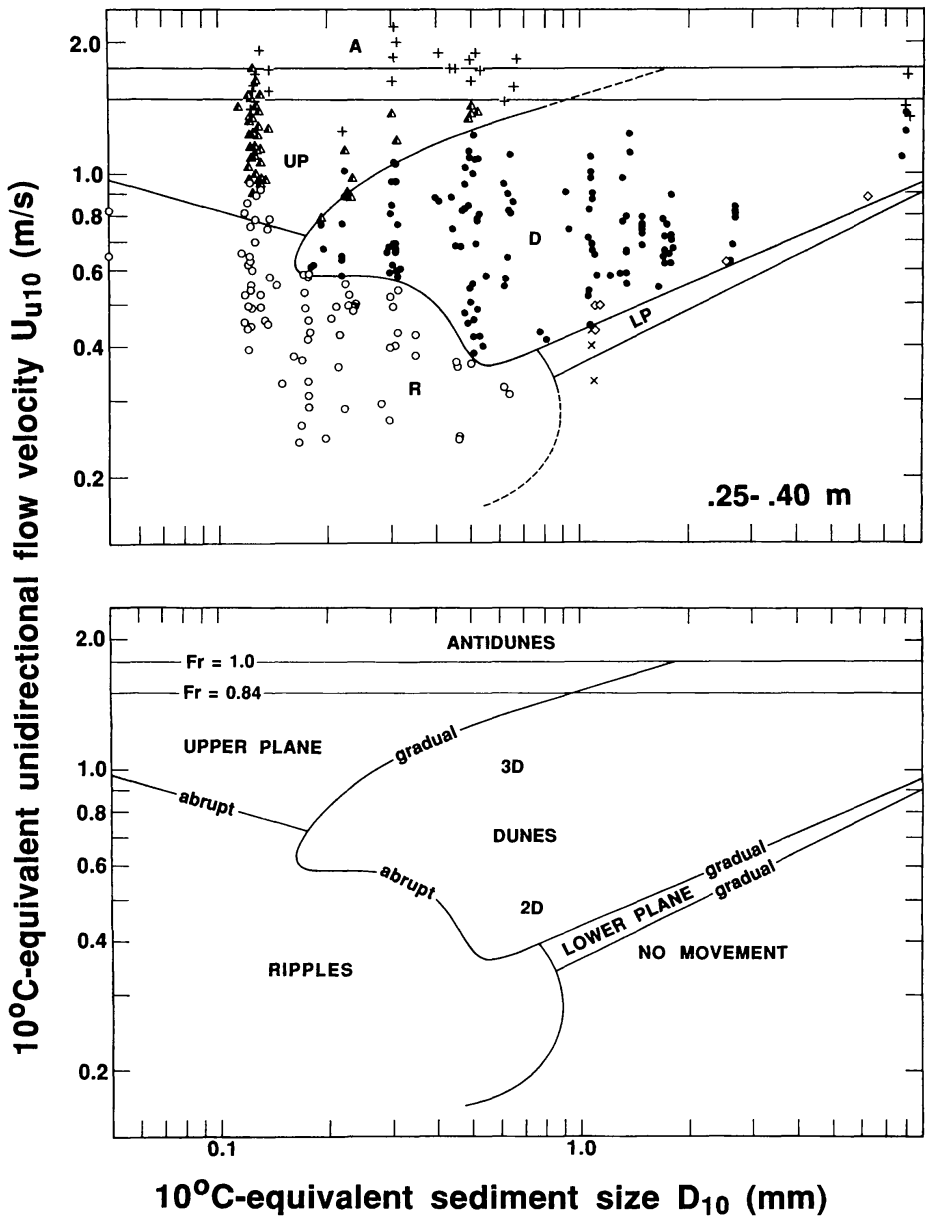

Figure 8 Relationships of unidirectional-flow bed-phase stability fields in a plot of U_{u10} vs D_{10} for flow depths d_{10} of 0.25–0.40 m in flumes. For data sources, see Southard & Boguchwal (1990). The *upper* graph shows the data, and the *lower* graph is schematic. The × 's indicate no movement on plane bed; other symbols and abbreviations defined in Figure 7 legend. Modified slightly from Southard & Boguchwal (1990); reproduced with permission of SEPM (Society for Sedimentary Geology).

to dunes with increasing U_{u10}, but in finer sediment, ripples give way (also abruptly) to plane beds. Although not well constrained, the ripple-plane boundary rises to higher U_{u10} with decreasing D_{10}.

Dunes are stable over a wide range of U_{u10} in sediments from medium sand to indefinitely coarse gravel. Both the lower and upper boundaries of the dune field rise with increasing U_{u10}, and both are gradual transitions rather than sharp breaks. For sediments coarser than about 0.8 mm, there is a narrow field below the dune field for a lower-regime plane bed; the lower boundary of this field is represented by the curve for threshold of sediment movement on a plane bed.

There is one triple point among ripples, dunes, and upper plane beds at a D_{10} of about 0.2 mm, and another among ripples, dunes, and lower plane beds at a D_{10} of about 0.8 mm. The coverage of data around these two triple points constrains the bed-phase relationships fairly closely. Between these two triple points the dune field forms a kind of indented salient pointing toward finer D_{10}. The boundary between ripples and upper plane beds seems to pass beneath the dune field at the upper-left triple point and emerges again at coarser D_{10} and lower U_{u10} as the boundary between ripples and lower plane beds at the lower-right triple point. Southard & Boguchwal (1990) speculate that the ripple-plane boundary is eclipsed by development of dunes on the bed over a certain range of U_{u10} and D_{10}. This interpretation has some experimental support: When the development of dunes is suppressed in very short channels, ripples persist to higher velocities. The stability fields for ripples and dunes thus seem to be controlled by dynamically separate effects, and the position of the boundary is mediated by the interaction between the two competing effects.

Velocity-size sections for other flow depths are qualitatively similar (Figure 9). With increasing flow depth, all phase boundaries shift upward (the antidune boundary the most rapidly), and the dune field spans a greater range of velocities. The sediment sizes associated with the two triple points seem to change little with flow depth.

Stress-Size Diagram

If τ_o instead of U_u is used to characterize bed states in unidirectional flows, the effect of d is much less. (A change in U_u with d for a given τ_o is no longer relevant, and all that is left is the smaller effect on τ_o of changes in bed-form geometry with d.) However, in some regions of the three-dimensional bed-phase diagram the one-to-one correspondence between locations in the diagram and sets of values of the dimensionless variables is lost, as noted in an earlier section. Therefore, a single suitably non-dimensionalized two-dimensional graph of τ_o against D should represent bed states reasonably well except for some overlap between certain bed-

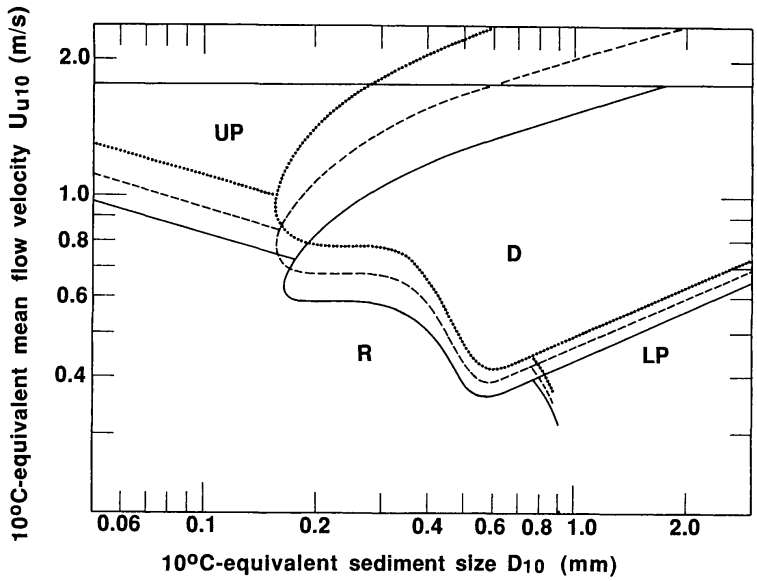

Figure 9 Changes in the positions of phase boundaries in velocity-size sections with flow depth. *Solid boundaries*, $d_{10} = 0.3$ m; *dashed boundaries*, $d_{10} = 1$ m; *dotted boundaries* (extrapolated to greater depth from flume work), $d_{10} = 3$ m. Abbreviations defined in Figure 7 legend. Modified slightly from Southard & Boguchwal (1990); reproduced with permission of SEPM (Society for Sedimentary Geology).

phase fields. Simons & Richardson (1966) first used this kind of plot, and the most recent and most comprehensive have been by Allen (1982, Vol. 1, pp. 339–40) and Southard & Boguchwal (1990).

Of the various ways of nondimensionalizing τ_o, a dimensionless boundary shear stress $\tau_o^\circ = (\rho/\mu^2\gamma'^2)^{1/3}$, standardized to a 10°C value τ_{o10} as before and also corrected to remove the sidewall contribution, is used here (cf Southard & Boguchwal 1990). This choice does not reflect the physics of flow and sediment movement as well as the conventional Shields parameter $\tau_o/\gamma' D$, but it has the practical advantage that τ_o and D do not appear in the same variable. Figures 10 and 11 show relations of bed phases in a graph of τ_{o10} against D_{10}; the data set is similar to that for Figures 7 and 8, although fewer data were usable because in some studies U_u was measured but not τ_o. Figure 10 shows all the data and field boundaries, and Figure 11 shows the fields and boundaries only schematically.

Scatter or overlapping of points for different bed phases is much greater in Figure 10 than in Figures 7 and 8. This is partly because of the unavoidably greater error in measuring τ_o than U_u, but in greater part because of the inherent ambiguity associated with τ_o: form resistance—the dominant contribution to τ_o over ripples and dunes—disappears in the transitions from ripples or dunes to upper plane beds, so τ_o actually decreases with increasing U_u in these transitions before increasing again. There is therefore

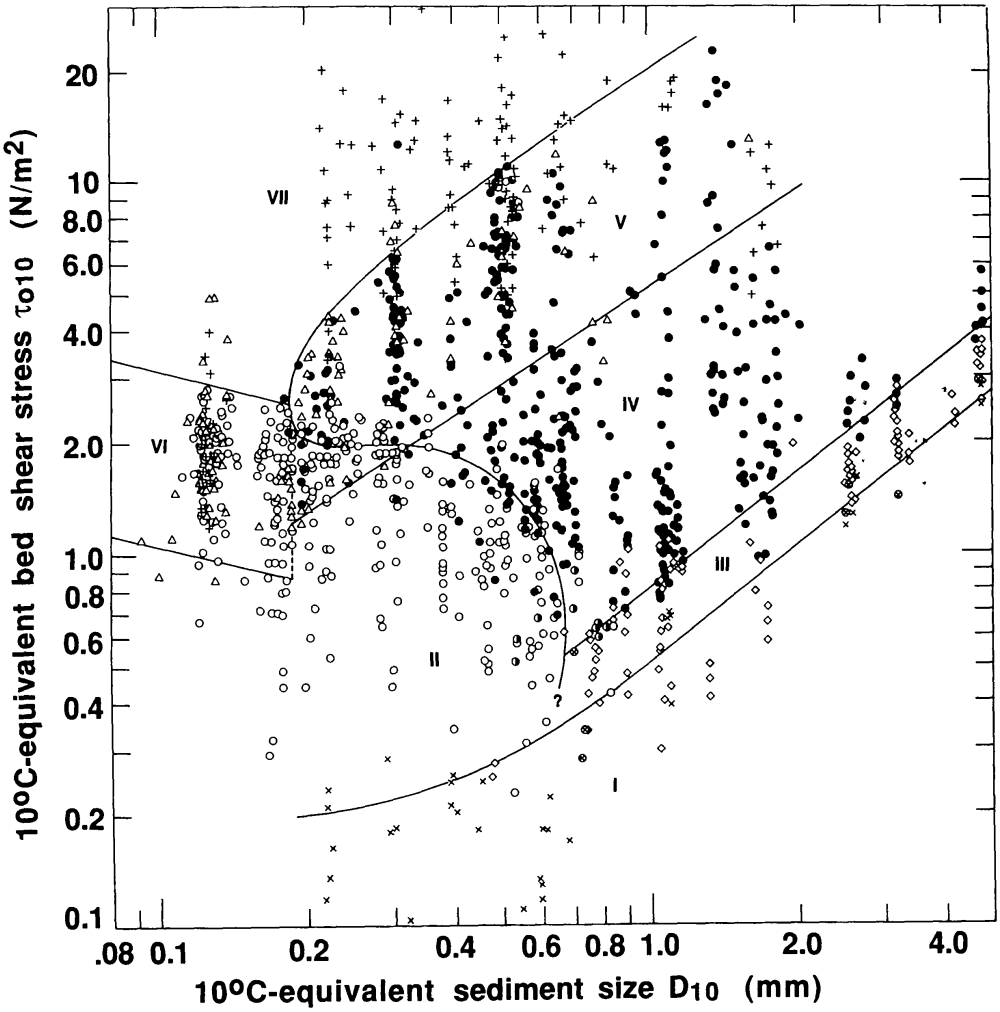

Figure 10 Relationships of unidirectional-flow bed-phase stability fields in a plot of t_{o10} vs D_{10} for a wide range of flow depths in flumes. For data sources, see Southard & Boguchwal (1990). The ×'s indicate no movement on plane bed; other symbols defined in Figure 7 legend. Labels for regions: I, no movement on plane bed; II, ripples; III, lower plane beds; IV, dunes; V, overlap region of dunes, upper plane beds, and antidunes; VI, overlap region of ripples, upper plane beds, and antidunes; VII, overlap region of upper plane beds and antidunes. Modified slightly from Southard & Boguchwal (1990); reproduced with permission of SEPM (Society for Sedimentary Geology).

a certain range of τ_o for which three different values of U_u are possible. In the plot of τ_{o10} vs D_{10} (Figure 10), this makes for an approximately horizontal band in which values of U_u, and the associated bed phases, overlap or fold onto one another. The greater scatter of data makes it more difficult to partition Figure 10 into bed-phase fields; partitioning was based in part on the more straightforward results for the d_{10}-U_{10}-D_{10} diagrams (Figures 7, 8).

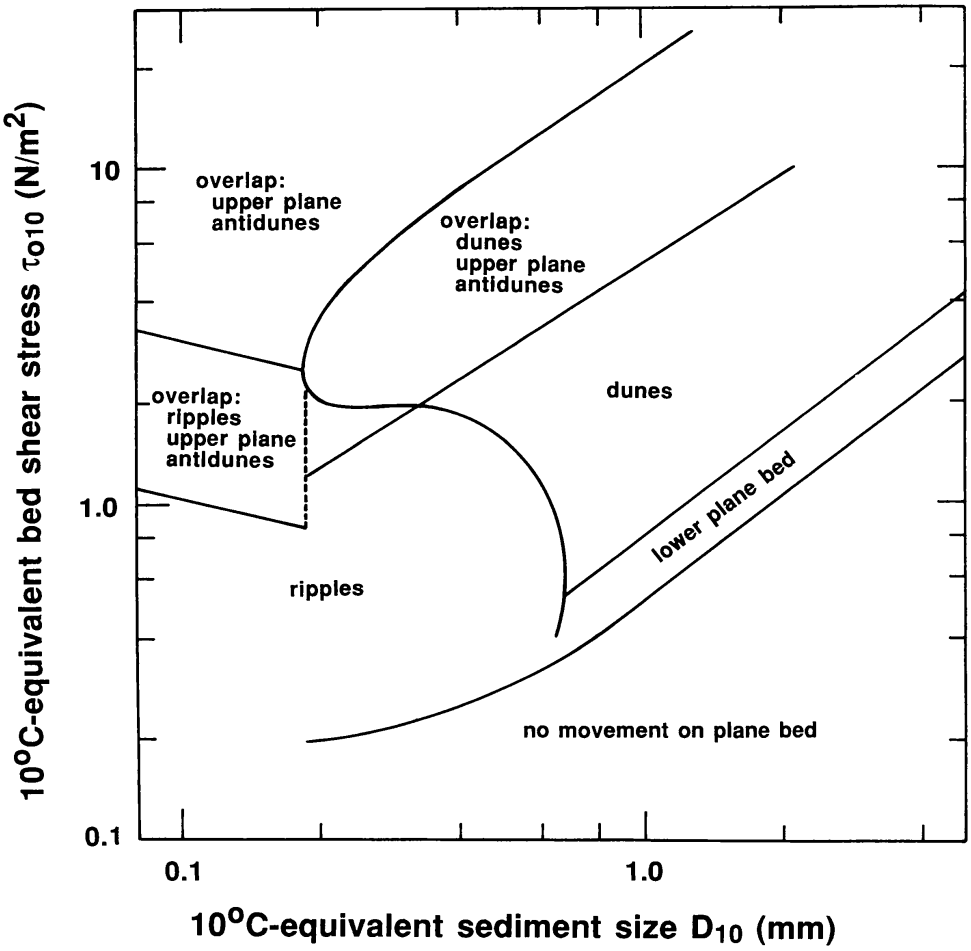

Figure 11 Schematic version of plot of t_{o10} vs D_{10} in Figure 10. Modified slightly from Southard & Boguchwal (1990); reproduced with permission of SEPM (Society for Sedimentary Geology).

Boundaries between no movement and lower-regime plane beds and between lower-regime plane beds and dunes in coarse sediments are analogous to those in Figure 8. Because of the moderate overlap of points, the boundary between ripples and dunes can be located only in a general way; its overall shape can be drawn to be qualitatively similar to that in Figure 8. This boundary must somehow continue downward past the question mark (Figure 10) and then leftward to define the minimum shear stress for the existence of ripples, but existing data are inadequate to define the position of this extension: It is not known whether it lies below the plane-bed threshold curve, as in Figure 8, or above it.

Interpretation of the other boundaries is based upon the existence of a minimum D_{10} in the range 0.15–0.20 mm for dunes (cf Figure 8) together with the effect of the τ_o ambiguity on the relations among ripples, dunes,

and upper plane beds. As in Figure 8, the ripple-dune boundary is shown to pass leftward through the vertical at the D_{10} minimum and then upward and to the right to become the dune-plane boundary. There is a wide range of τ_{o10} below this latter boundary for which either ripples or dunes are possible, depending upon how the flow conditions were originally established. The lower limit of this region, whose position is not well constrained, must terminate leftward at the D_{10} dune minimum and so is shown connected upward to that point by a vertical dashed line.

To the left of the D_{10} dune minimum, ripples pass directly into upper plane beds, again with a broad overlap region whose upper and lower limits are poorly constrained. The line representing the upper limit for ripples is shown to end at the point of vertical tangent to the dune boundary, at the D_{10} dune minimum, but it could just as well end somewhat above or somewhat below that point. In any case, the other of these boundaries, giving the lower limit for the existence of upper plane beds, must end to the right at the same sediment size—hence the vertical dashed line connecting the two boundaries. Since the intersection should not be expected to be exactly at the minimum sediment size for dunes, this vertical dashed line should actually be at a slightly different and greater sediment size from that of the vertical dashed line (mentioned above) connecting the two analogous curves for dunes at greater sediment sizes. So there must really be *two* vertical dashed lines, very close together. Existing data cannot fix the position of these two lines.

Antidune points are widely scattered in the upper part of Figure 9, for two reasons: (*a*) The transition between plane beds and antidunes with increasing U_{u10} at the usual flow depths of flumes is at values of τ_{o10} that are even smaller than the maximum τ_{o10} for dunes, and (*b*) the minimum τ_{o10} for antidunes increases with d, and a wide range of d is combined into Figure 10. Other effects of flow depth on the positions of the various boundaries in τ_{o10}-D_{10} plots are so minor as to be swamped by the data scatter.

BED CONFIGURATIONS IN OSCILLATORY FLOWS

General

Oscillatory flows over sediment beds are easily made in the laboratory, in three ways. First, real waves can be made with wave generators of various kinds in open tanks and basins. Many such experiments have been performed, although mostly with simple monochromatic waves in relatively narrow tanks; although technically feasible, little work seems to have been done on bed configurations under more complex waves with a spectrum of periods and directions in wide basins. Even aside from the inevitable

problem of reflected waves, the maximum wave period is severely limited by the size of the tank or basin, and few experiments have been made at periods greater than 3–4 s.

Oscillatory flows with a wide range of periods and speeds are also easily made in oscillatory-flow ducts, in which the water is driven back and forth in approximately simple harmonic motion in various ways over the sediment bed through a closed duct between reservoirs at the ends. Such experiments are necessarily limited to bidirectional oscillations. Experiments up to now have been limited to single-component oscillations, but a successful beginning has been made with multicomponent oscillations (W. L. Duke, personal communication). The natural period increases with duct length, so long ducts are needed to simulate long-period waves; although the practical constraints are not as serious as for wave tanks, only Southard et al (1990) have made experiments at periods of greater than 6–7 s in a long, wide duct. The spatial velocity field at a given time, both inside and outside the oscillatory boundary layer, is not exactly the same as under real waves, but the bed configurations produced are very much like those generated in open wave tanks.

Finally, bed configurations can be made in a tank of still water by oscillating a submerged planar horizontal tray covered with sediment. The relative motion of the fluid and the sediment is grossly the same, although there are differences in fluid and particle accelerations. Only three such sets of experiments have been reported (Bagnold 1946, Manohar 1955, Sleath 1976), all using fairly short oscillation periods.

Comparison of results from the three different arrangements (Miller & Komar 1980b) suggests that wave tanks and oscillatory-flow tunnels give not greatly different results but that oscillating-bed tanks give rather different results. The summary in the following section therefore uses data only from wave tanks and flow ducts.

Only experimental results on oscillatory-flow bed configurations are considered here. For recent field studies in necessarily more complex flow environments, following upon Inman's (1957) classic field study, see Inman & Dingler (1976), Miller & Komar (1980a), Davies (1985), Boyd et al (1985), Kos'yan (1988), and Amos et al (1988), among others.

Period-Speed-Size Diagram

Harms et al (1982) reviewed the geometry and hydraulic relationships of oscillatory-flow bed states in the framework of the period-speed-size diagram. This section presents an updated version of that review, based on eight studies published in the accessible literature in which bed geometry, water temperature, and flow and sediment variables were reported. The results are shown as U_{o10}-T_{10} graphs for two different narrow

ranges of D_{10}: 0.10–0.20 mm (Figure 12) and 0.50–0.65 mm (Figure 13). Shown also in Figures 12 and 13 are lines of equal orbital diameter d_o, sloping downward to the right. A striking feature of Figures 12 and 13 is the scarcity of data points for oscillation periods greater than 6–8 s, precisely the range of greatest importance for interpreting the sedimentary record. Conclusions must therefore remain tentative until more work is done at these longer periods.

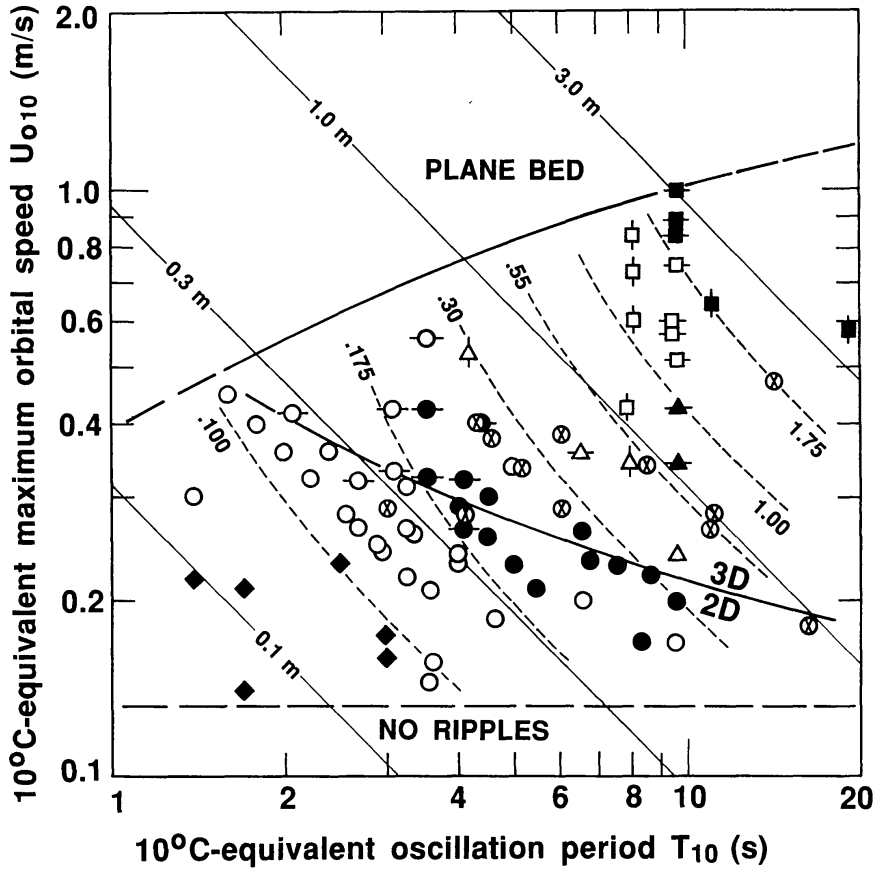

Figure 12 Relationships of oscillatory-flow bed configurations in plots of U_{o10} against T_{10} for D_{10} values of 0.10–0.20 mm in oscillatory-flow tanks and ducts. Symbolism for ripple spacing: *solid diamonds*, <0.100 m; *open circles*, 0.10–0.175 m; *solid circles*, 0.175–0.30 m; *open triangles*, 0.30–0.55 m; *solid triangles*, 0.55–1.00 m; *open squares*, 1.00–1.75 m; *solid squares*, >1.75 m. Horizontal tick marks indicate a three-dimensional (3D) configuration; symbols without tick marks represent a two-dimensional (2D) configuration, except that circles with enclosed ×'s represent a three-dimensional configuration for which a characteristic ripple spacing was not measured. Vertical tick marks indicate ripples whose spacing is much greater than the duct width, so that the three-dimensional geometry of the ripples could not be observed. Data sources: Yalin & Russell (1963), Inman & Bowen (1963), Kennedy & Falcón (1965), Carstens et al (1969), Mogridge & Kamphuis (1972), Dingler (1974), Miller & Komar (1980), and Southard et al (1990).

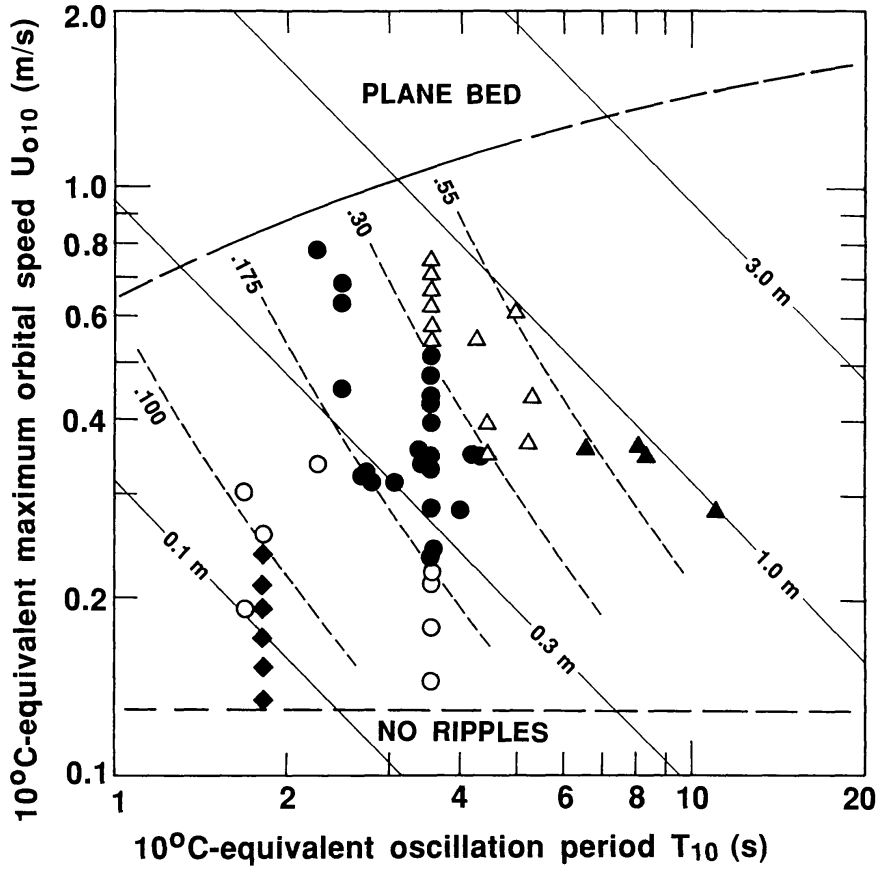

Figure 13 Relationships of oscillatory-flow bed configurations in plots of U_{o10} against T_{10} for D_{10} values of 0.50–0.65 mm in oscillatory-flow tanks and ducts. Symbols and data sources are the same as in Figure 12.

In Figures 12 and 13 a broad field of ripples of various sizes and shapes is bounded below by a field in which the flow is too weak to maintain equilibrium ripples and above by a field for transport over a planar bed. The boundary between ripples and plane beds is clear-cut, but because of the scarcity of official plane-bed data points (not shown), it is fairly well constrained only at intermediate oscillation periods. The boundary between ripples and no ripple maintenance is less well defined owing to a lack of well-documented runs. This boundary is drawn arbitrarily to be horizontal. As in the unidirectional case, there actually are two boundaries in this region of the graph—one for development of ripples on a planar bed and the other for maintenance of preexisting ripples with slowly decreasing velocity. The ripple field clearly broadens rightward. The minimum period for generation of ripples seems not to have been studied, but in any case it is unimportant for natural sedimentary environments.

In Figure 12, for very fine to fine sand, ripple spacings increase from

about 0.05 m at periods of less than 2 s to well over a meter at periods approaching 10 s. Crude contours of spacing, drawn where possible, are nearly parallel to lines of equal orbital diameter d_o, reflecting the well-known tendency for oscillatory-flow ripples to scale with orbital diameter; there seems, however, to be a tendency for these contours to be steeper than the lines of constant d_o. The outstanding feature of this graph is a transition from regular and straight-crested ripples (two-dimensional ripples) at low oscillatory speeds and small periods to irregular (three-dimensional ripples) at high oscillatory speeds and long periods. This transition has been reported in several studies but has not been studied in detail. Ripple spacings in some of these three-dimensional ripple runs were not even approximately reported. At the longest oscillation periods typical of shallow marine environments, in the range 8–20 s, large three-dimensional ripples are the stable configuration at oscillation speeds up to about 1 m s^{-1}.

It is clear that all of the two-dimensional ripples, at relatively small U_{u10}, are oscillatory-current ripples, as defined in an earlier section. The onset of three-dimensional geometry with increasing U_{u10} at any given T_{10} seems to reflect the development of reversing-current ripples (which are dynamically akin to current ripples in unidirectional flows and vary little in spacing) and their increasingly strong interaction with the oscillatory-current ripples. At longer T_{10} and even greater U_{u10} the oscillatory-current ripples grow to be much larger than the reversing-current ripples, thus eliminating the strong interaction between the two; the reversing-current ripples are only passively superimposed upon these larger oscillatory-current ripples. It is to be emphasized that much more work must be done at relatively large U_{u10} and T_{10} before these speculative relationships can be confirmed.

Careful observations of oscillation ripples in the shallow oceans, most notably by Inman (1957), have revealed the existence at moderate to large oscillation speeds and long oscillation periods (see upper right of Figure 12) of only small two-dimensional ripples, with spacings almost without exception in the range 0.07–0.08 m, rather than large three-dimensional ripples. These small ripples are almost certainly reversing-current ripples, described above. Why were large three-dimensional ripples not observed? Was not enough time available as the oscillatory flow waned from plane-bed conditions? Or is there something inherent in oscillatory flow in a closed flow duct that is conducive to their development? The ancient sedimentary record of shallow-marine environments gives incontrovertible evidence of large-scale three-dimensional oscillation ripples in fine sands, but we have no way of knowing whether the oscillatory flow was dominated by a single component or was instead composed of a range of components

with different periods, directions, and amplitudes. Only observations of the bed configuration in the shallow ocean during storms can resolve this question.

Relationships of ripples in coarse sands, shown in Figure 13, are simpler than in fine sands. Ripple spacing again increases upward to the right, scaled closely to orbital diameter. Again the crude contours of equal ripple spacing seem to slope a little more steeply than the lines of constant d_o. Somewhat surprisingly, the lower boundary of the ripple field seems to be in about the same position as for the much finer sands. All of the ripples are two-dimensional oscillatory-current ripples; for reasons unclear, the instability leading to three-dimensional geometry in fine sands is not manifested in coarse sands. Neither are large three-dimensional oscillation ripples represented in the ancient sedimentary record.

BED CONFIGURATIONS IN COMBINED FLOWS

Combined flows are most easily made in the laboratory in three ways: (*a*) by superimposing a current on an oscillatory flow in a wave tank; (*b*) by superimposing a current on an oscillatory flow in a closed duct; or (*c*) by superimposing wind-generated waves on a current in a recirculating channel. Only in the second case can a wide range in both U_o and U_u as well as in T be attained. If the tank or duct is very wide, waves and currents can be generated at an arbitrary angle, but studies up to now have been made only in narrow tanks and ducts, for which the oscillatory and unidirectional components are parallel. Even more general combined flows with a multicomponent oscillatory component represent a formidable experimental problem, and no such work has yet been reported. There has been little work even in simple rectilinear combined flows; the most extensive data set so far is that of Arnott & Southard (1990), in which only a single period and sediment size were used. Further work on combined-flow bed forms certainly represents the greatest present need in experimental studies on bed states.

It was pointed out in an earlier section that representing bed states in a three-dimensional graph is not as natural for combined flows as for purely oscillatory or unidirectional flows because, in general, neither flow depth nor oscillation period can be neglected. Since the few available experimental data on bed states in combined flows are for oscillation-dominated flows, we here adopt the approximate but qualitatively reasonable expedient of attempting to view three-dimensional sections through a four-dimensional U_u-U_o-T-D diagram. Systematic experimental data on combined-flow bed states are so limited that at present this amounts to nothing more

than looking at a single U_u-U_o section for single values of period and sediment size.

Figure 14, based on experiments by Arnott & Southard (1990), shows relationships of combined-flow bed phases in a U_{o10}-U_{u10} graph for a single sand size ($D_{10} = 0.09$ mm) and a single oscillation period ($T_{10} = 9.5$ s). Owing to limitations on pumping capacity, only oscillation-dominated flows, with U_{u10} less than 0.25 m s^{-1}, were studied. Few other laboratory data are yet available: The only other work done so far has been with small-scale ripples at short oscillation periods (Inman & Bowen 1963, Harms 1969, Brevik & Aas 1980).

The U_{o10}-U_{u10} plot in Figure 14 is partitioned into fields for various intergradational bed phases. In the range of flows studied ($U_{o10} = 0$–0.80 m s^{-1}, $U_{u10} = 0$–0.25 m s^{-1}) these bed phases are no movement, small two-dimensional ripples, small three-dimensional ripples, large three-dimensional ripples, and plane beds. The transitions among these bed phases are gradual; the partitioning is only an attempt to identify

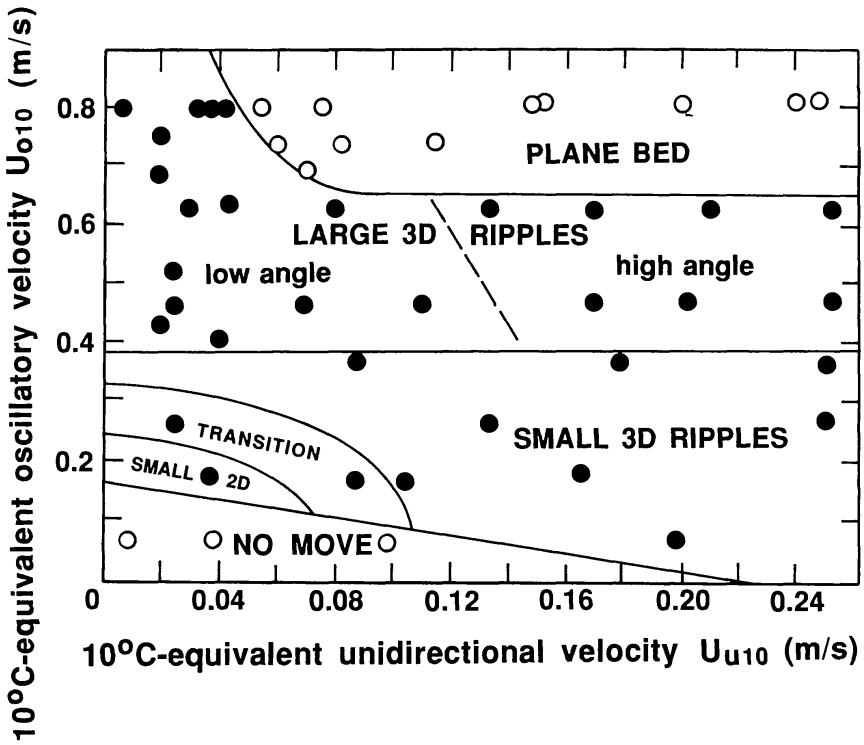

Figure 14 Relationships of combined-flow bed configurations in a plot of U_{o10} against U_{u10} for a D_{10} value of 0.09 mm and a T_{10} value of 9.5 s in a combined-flow duct. *Solid circles*, combined-flow ripples; *open circles*, no sediment movement on a plane bed (above the ripple field) or no sediment movement (below the ripple field). Modified slightly from Arnott & Southard (1990); reproduced with permission from SEPM (Society for Sedimentary Geology).

regions with distinctive bed geometry and is not meant to imply sharp distinctions among the various phases. But the differences in bed configuration from region to region in Figure 14 are real and substantial. In particular, the transition from small ripples to large ripples seems to represent a region of accelerated change in bed-form scale compared with regions above and below, where changes, although not negligible, are slower.

The sequence of bed phases along the U_{o10} axis is known from one earlier study (Southard et al 1990) using the same D_{10} and T_{10}: No movement, small two-dimensional ripples, small three-dimensional ripples, large three-dimensional ripples, plane beds. Likewise, the sequence of bed phases along the U_{u10} axis is well known from many studies in unidirectional flow: no movement, unidirectional-flow ripples, plane beds. In the interior of the graph, the boundary between no movement and combined-flow ripples is not well constrained and is shown arbitrarily as a straight line. The boundary between combined-flow ripples and plane beds, on the other hand, is fairly well constrained: Within the range of U_{u10} attainable, it falls sharply with U_{u10} at first and then becomes nearly horizontal.

Over a narrow range of U_{o10} above threshold and for very small U_{u10} (less than a few centimeters per second) the bed configuration consists of regular ripples with straight and laterally continuous sharp crests and broad troughs oriented perpendicular to the flow. Ripple profiles are only slightly asymmetrical. With only a slight increase in either of the velocity components, the ripples become increasingly irregular in plan geometry. Rightward from the U_{o10} axis, over the entire range of U_{u10} studied, the configuration consists of relatively small ripples with more or less sinuous (although fairly continuous) crest lines and with more or less pronounced local lows or scour pits in troughs. Dips on the upstream and downstream ripple flanks are not greatly different, but the lamination within the ripples always dips downstream because the ripples move slowly in the direction of the unidirectional component. Even at small values of U_{u10}, the overall appearance of the ripples is not grossly different from those in purely unidirectional flows.

As U_{o10} increases beyond about 0.4 m s^{-1}, the three-dimensional ripples become much larger. The transition is gradual, but the rate of change with increasing U_{o10} is greater than at smaller U_{o10}. Bed-form crests become less continuous and more rounded, resulting in forms whose geometry could be described as hummocky. As spacing continues to increase to over 2 m at the highest values of U_{o10}, detailed information on plan geometry is lost owing to the narrowness of the flow duct used, although the ripples are still substantially three dimensional. Except at the greatest U_{o10}, small

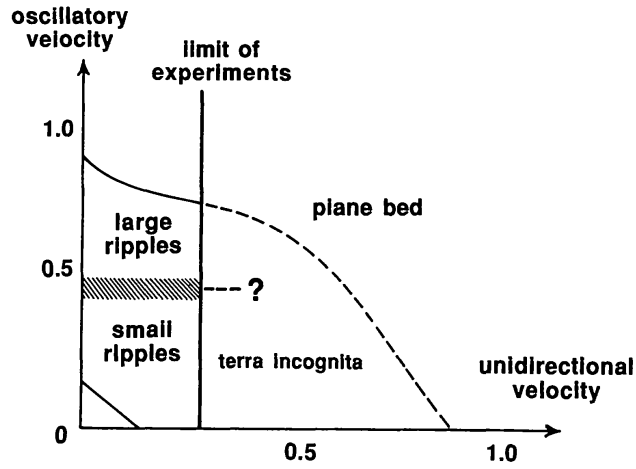

Figure 15 Speculative extrapolation of the U_{o10}-U_{u10} plot in Figure 14 to greater values of the unidirectional velocity component.

reversing-current ripples are prominently superimposed. With increasing U_{u10} the flow-parallel profiles of the three-dimensional ripples become more asymmetrical, eventually attaining lee-side angles of up to 25°. A unidirectional component of only a few centimeters per second is needed to make the profiles noticeably asymmetrical. Heights first increase with U_{o10} and then decrease in the transition to plane beds. Spacings are a large percentage of the orbital diameter, suggesting that these large three-dimensional ripples are analogues of the orbital (vortex) ripples well known from oscillatory flows.

These large three-dimensional combined-flow ripples must somehow disappear with increasing U_{u10}, because in purely unidirectional flow small three-dimensional ripples pass into plane beds with increasing velocity, and the upper boundary of combined-flow ripples must connect with that transition point on the U_{u10} axis (Figure 15). Also to be ascertained is the relationship between large combined-flow ripples in very fine sand, like those described above, and dunes in purely unidirectional flow in sands coarser than about 0.2 mm. A whole series of intermediate "sections" in the U_o-U_u-D-T graph must be explored to establish this relationship, even for the simplest case of combined flow, in which the oscillatory and unidirectional components are parallel. Designing and testing apparatus for studying such relationships in more general combined flows, which are of such great relevance to natural flow environments, is one of the most challenging tasks facing experimental physical sedimentologists today.

Literature Cited

Allen, J. R. L. 1974. Reaction, relaxation and lag in natural sedimentary systems: general principles, examples and lessons. *Earth Sci. Rev.* 10: 263–342

Allen, J. R. L. 1976a. Bed forms and unsteady processes: some concepts of classification and response illustrated by common one-way types. *Earth Surf. Processes* 3: 361–74

Allen, J. R. L. 1976b. Computational models for dune time-lag: general ideas, difficulties, and early results. *Sediment. Geol.* 15: 1–53

Allen, J. R. L. 1982. *Sedimentary Structures: Their Character and Physical Basis*, Vols. 1, 2. Amsterdam: Elsevier. 593 pp., 663 pp.

Amos, C. L., Bowen, A. J., Huntley, D. A., Lewis, C. F. M. 1988. Ripple generation under the combined influence of waves and currents on the Canadian continental shelf. *Cont. Shelf Res.* 8: 1129–53

Arnott, R. W., Southard, J. B. 1990. Experimental study of combined-flow bed configurations in fine sands, and some implications for stratification. *J. Sediment. Petrol.* 60: 211–19

Ashley, G. M. 1990. Classification of large-scale subaqueous bed forms: a new look at an old problem. SEPM Bedforms and Bedding Structures Research Symposium. *J. Sediment. Petrol.* 60: 160–72

Bagnold, R. A. 1946. Motion of waves in shallow water. Interaction of waves and sand bottoms. *Proc. R. Soc. London Ser. A* 187: 1–15

Boyd, R., Forbes, D. L., Heffler, D. E. 1985. Time-sequence observations of wave-formed sand ripples on an ocean shoreface. *Sedimentology* 35: 449–64

Brevik, I., Aas, B. 1980. Flume experiments on waves and currents. *Coast. Eng.* 3: 149–77

Brooks, N. H. 1958. Mechanics of streams with movable beds of fine sand. *Trans. Am. Soc. Civ. Eng.* 123: 536–49

Brownlie, W. R. 1981. Prediction of flow depth and sediment discharge in open channels. *Rep. No. KH-R-43A*, Keck Lab. Hydraul. and Water Resour., Calif. Inst. Technol., Pasadena. 232 pp.

Buckingham, E. 1914. On physically similar systems; illustrations of the use of dimensional equations. *Phys. Rev.* 4: 354–76

Carstens, M. R., Neilson, F. M. 1967. Evolution of a duned bed under oscillatory flow. *J. Geophys. Res.* 72: 3053–59

Carstens, M. R., Neilson, F. M., Altinbilek, H. D. 1969. Bed forms generated in the laboratory under oscillatory flow: analytical and experimental study. *US Army Corps Eng., Coast. Eng. Res. Cent., Tech. Memo. 28*. 39 pp.

Chabert, J., Chauvin, J. L. 1963. Formation des dunes at des rides dans les modèles fluviaux. *Lab. Natl. d'Hydraul., Cent. Rech. et d'Essais de Chatou, Bull.* 4: 31–51

Clifton, H. E. 1976. Wave-formed sedimentary structures—a conceptual model. In *Beach and Nearshore Sedimentation. SEPM Spec. Publ. No. 24*, ed. R. A. Davis, R. L. Ethington, pp. 126–48. Tulsa: Soc. Econ. Paleontol. Mineral.

Clifton, H. E., Dingler, J. R. 1984. Wave-formed structures and paleoenvironmental reconstruction. *Mar. Geol.* 60: 165–98

Clifton, H. E., Hunter, R. E., Phillips, R. L. 1971. Depositional structures and processes in the nonbarred high energy nearshore. *J. Sediment. Petrol.* 41: 651–70

Costello, W. R., Southard, J. B. 1981. Flume experiments on lower-flow-regime bed forms in coarse sand. *J. Sediment. Petrol.* 51: 849–64

Davies, A. G. 1985. Observations of the stability of oscillatory flow above the seabed and of sand ripple formation. *Cont. Shelf Res.* 4: 553–80

Dingler, J. R. 1974. *Wave-formed ripples in nearshore sands*. PhD thesis. Univ. Calif. at San Diego, La Jolla. 136 pp.

Engelund, F., Fredsøe, J. 1982. Sediment ripples and dunes. *Annu. Rev. Fluid Mech.* 14: 13–37

Fredsøe, J. 1979. Unsteady flow in straight alluvial streams: modification of individual dunes. *J. Fluid Mech.* 91: 497–512

Fredsøe, J. 1981. Unsteady flow in straight alluvial streams. Part 2. Transition from dunes to plane bed. *J. Fluid Mech.* 102: 431–53

Gee, D. M. 1975. Bed form response to nonsteady flows. *Am. Soc. Civ. Eng., J. Hydraul. Div.* 101: 437–49

Gilbert, G. K. 1914. The transportation of debris by running water. *US Geol. Surv. Prof. Pap. 86*. 263 pp.

Guy, H. P., Simons, D. B., Richardson, E. V. 1966. Summary of alluvial channel data from flume experiments, 1956–1961. *US Geol. Surv. Prof. Pap. 462-I*. 96 pp.

Harms, J. C. 1969. Hydraulic significance of some sand ripples. *Geol. Soc. Am. Bull.* 80: 363–96

Harms, J. C. 1979. Primary sedimentary structures. *Annu. Rev. Earth Planet. Sci.* 7: 227–48

Harms, J. C., Southard, J. B., Walker, R. G. 1982. *Structures and Sequences in Clastic*

Rocks. SEPM Short Course No. 9. Tulsa: Soc. Econ. Paleontol. Mineral. 253 pp.
Hayashi, T., Onishi, M. 1983. Dominant wave numbers of ripples, dunes and antidunes on alluvial river beds. *Proc. Int. Symp. River Sediment., 2nd, Nanjing, China*
Inman, D. L. 1957. Wave-generated ripples in nearshore sands. *US Army Corps Eng., Beach Eros. Board, Tech. Memo. 100.* 41 pp.
Inman, D. L., Bowen, A. J. 1963. Flume experiments on sand transport by waves and currents. *Proc. Coast. Eng. Conf., 8th, Am. Soc. Civ. Eng.*, pp. 137–50
Inman, D. L., Dingler, J. R. 1976. Wave-formed ripples in nearshore sands. *Proc. Coast. Eng. Conf., 15th, Am. Soc. Civ. Eng.*, pp. 2109–26
Kaneko, A., Honji, H. 1979a. Initiation of ripple marks under oscillating water. *Sedimentology* 26: 101–13
Kaneko, A., Honji, H. 1979b. Double structure of viscous flow over a wavy wall. *J. Fluid Mech.* 93: 727–36
Kennedy, J. F. 1961. Further laboratory studies of the roughness and suspended load of alluvial streams. *Rep. No. KH-R-3*, Keck Lab. Hydraul. and Water Resour., Calif. Inst. Technol., Pasadena. 36 pp.
Kennedy, J. F., Brooks, N. H. 1963. Laboratory study of an alluvial stream at constant discharge. *Proc. Fed. Inter-Agency Sediment. Conf. US Dep. Agric., Agric. Res. Serv., Misc. Publ. 970*, pp. 320–30
Kennedy, J. F., Falcón, M. 1965. Wave-generated sediment ripples. *Rep. No. 86*, Hydrodyn. Lab., Mass. Inst. Technol., Cambridge. 55 pp.
Kobayashi, N., Madsen, O. S. 1985. Formation of ripples in erodible channels. *J. Geophys. Res.* 90: 7332–40
Komar, P. D. 1974. Oscillatory ripple marks and the evaluation of ancient wave conditions and environments. *J. Sediment. Petrol.* 44: 169–80
Kos'yan, R. D. 1988. Study of sediment microforms in the nearshore zone. *Mar. Geol.* 83: 63–78
Laboratoire National d'Hydraulique, Centre de Recherches et d'Essais de Chatou. 1961. Etude general des matériaux de fond mobile. *Rapp. No. 1*
Langbein, W. B., Leopold, L. B. 1968. River channel bars and dunes—theory of kinematic waves. *US Geol. Surv. Prof. Pap. 422-L.* 20 pp.
Lofquist, K. E. B. 1978. Sand-ripple growth in an oscillatory-flow water tunnel. *US Army Corps Eng., Coast. Eng. Res. Cent., Tech. Pap. 78-5.* 101 pp.
Longuet-Higgins, M. S. 1981. Oscillating flow over steep sand ripples. *J. Fluid Mech.* 107: 1–35
Manohar, M. 1955. Mechanics of bottom sediment movement due to wave action. *US Army Corps Eng., Beach Eros. Board, Tech. Memo. 75.* 121 pp.
Middleton, G. V., Southard, J. B. 1984. *Mechanics of Sediment Movement. SEPM Short Course No. 3.* Tulsa, Okla: Soc. Econ. Paleontol. Mineral. 401 pp. 2nd ed.
Miller, M. C., Komar, P. D. 1980a. A field investigation of the relationship between oscillation ripple spacing and the near-bottom water orbital motions. *J. Sediment. Petrol.* 50: 183–91
Miller, M. C., Komar, P. D. 1980b. Oscillation sand ripples generated by laboratory apparatus. *J. Sediment. Petrol.* 50: 173–82
Miller, M. C., McCave, I. N., Komar, P. D. 1977. Threshold of sediment motion under unidirectional currents. *Sedimentology* 24: 507–27
Mogridge, G. R., Kamphuis, J. W. 1972. Experiments on bed form generation by wave action. *Proc. Coast. Eng. Conf., 13th, Am. Soc. Civ. Eng.* 2: 1123–42
Nielsen, P. 1981. Dynamics and geometry of wave-generated ripples. *J. Geophys. Res.* 86: 6467–72
Nordin, C. F. Jr. 1976. Flume studies with fine and coarse sands. *US Geol. Surv. Open-File Rep. 76-762.* 18 pp.
Pratt, C. J. 1971. *An experimental investigation into the flow of water and the movement of bed material in alluvial channels.* PhD thesis. Univ. Southampton, Engl. 209 pp.
Richards, K. J. 1980. The formation of ripples and dunes on an erodible bed. *J. Fluid Mech.* 99: 597–618
Rubin, D. M., McCulloch, D. S. 1980. Single and superimposed bedforms: a synthesis of San Francisco Bay and flume observations. *Sediment. Geol.* 26: 207–31
Rubin, D. M., Hunter, R. E. 1987. Bedform alignment in directionally varying flows. *Science* 237: 276–78
Simons, D. B., Richardson, E. V. 1962a. The effect of bed roughness on depth-discharge relations in alluvial channels. *US Geol. Surv. Water-Supply Pap. 1498-E.* 26 pp.
Simons, D. B., Richardson, E. V. 1962b. Depth-discharge relations in alluvial channels. *Am. Soc. Civ. Eng., J. Hydraul. Div.* 88(5): 57–72
Simons, D. B., Richardson, E. V. 1963. Forms of bed roughness in alluvial channels. *Trans. Am. Soc. Civ. Eng.* 128(I): 284–302
Simons, D. B., Richardson, E. V. 1966. Resistance to flow in alluvial channels. *US Geol. Surv. Prof. Pap. 422-J.* 61 pp.

Simons, D. B., Richardson, E. V., Albertson, M. L. 1961. Flume studies using medium sand. *US Geol. Surv. Water-Supply Pap. 1498-A*. 76 pp.
Sleath, J. F. A. 1975. A contribution to the study of vortex ripples. *J. Hydraul. Res.* 13: 315–28
Sleath, J. F. A. 1976. On rolling-grain ripples. *J. Hydraul. Res.* 14: 69–81
Song, C. C. S. 1983. Modified kinematic model: applications to bed forms. *J. Hydraul. Eng.* 109: 1133–51
Sorby, H. C. 1859. On the structures produced by the currents present during the deposition of stratified rocks. *The Geologist* 2: 137–47
Sorby, H. C. 1908. On the application of quantitative methods to the study of the structure and history of rocks. *Q. J. Geol. Soc. London* 64: 171–233
Southard, J. B., Boguchwal, L. A. 1990. Bed configurations in steady unidirectional water flows. Part 2. Synthesis of flume data. *J. Sediment. Petrol.* 60(5): 658–79
Southard, J. B., Boguchwal, L. A., Romea, R. D. 1980. Test of scale modelling of sediment transport in steady unidirectional flow. *Earth Surf. Processes* 5: 17–23
Southard, J. B., Lambie, J. M., Federico, D. C., Pile, H. T., Weidman, C. R. 1990. Experiments on bed configurations in fine sands under bidirectional purely oscillatory flow, and the origin of hummocky cross-stratification. *J. Sediment. Petrol.* 60: 1–17
Stein, R. A. 1965. Laboratory studies of total load and apparent bed load. *J. Geophys. Res.* 70: 1831–42
Sumer, B. M., Bakioglu, M. 1984. On the formation of ripples on an erodible bed. *J. Fluid Mech.* 144: 177–90
Vanoni, V. A., Brooks, N. H. 1957. Laboratory studies of the roughness and suspended load of alluvial streams. *Rep. No. E-68*, Sediment. Lab., Calif. Inst. Technol., Pasadena (also *US Army Corps Eng., Missouri River Div., Sediment Ser. 11*. 121 pp.)
Vanoni, V. A., ed. 1975. *Sedimentation Engineering*. New York: Am. Soc. Civil Eng. 745 pp.
Vongvisessomjai, S. 1984. Oscillatory ripple geometry. *J. Hydraul. Eng.* 110: 247–66
Williams, G. P. 1967. Flume experiments on the transport of a coarse sand. *US Geol. Surv. Prof. Pap. 562-B*. 31 pp.
Williams, G. P. 1970. Flume width and water depth effects in sediment-transport experiments. *US Geol. Surv. Prof. Pap. 562-H*. 37 pp.
Willis, J. C., Coleman, N. L., Ellis, W. M. 1972. Laboratory study of transport of fine sand. *Am. Soc. Civ. Eng., J. Hydraul. Div.* 98: 489–502
Yalin, M. S., Russell, R. C. H. 1963. Similarity in sediment transport due to waves. *Proc. Coast. Eng. Conf., 8th, Am. Soc. Civ. Eng.*, pp. 151–67

LIST OF SYMBOLS

D	Median sediment size
d	Mean flow depth
D_{10}	Median sediment size standardized to 10°C water temperature
d_{10}	Mean flow depth standardized to 10°C water temperature
D°	Dimensionless median sediment size
d°	Dimensionless mean flow depth
d_{o}	Orbital diameter
D_{r}	Ratio of two sediment sizes
d_{r}	Ratio of two flow depths
g	Acceleration of gravity
P	Flow power
q	Discharge per unit width of flow
T	Oscillation period
T_{10}	Oscillation period standardized to 10°C water temperature
T°	Dimensionless oscillation period

T_r Ratio of two oscillation periods
U_o Oscillatory component of flow velocity
U_{o10} Oscillatory component of flow velocity standardized to 10°C water temperature
U_o° Dimensionless oscillatory component of flow velocity
U_r Ratio of two flow velocities
U_u Unidirectional component of flow velocity
U_{u10} Unidirectional component of flow velocity standardized to 10°C water temperature
U_u° Dimensionless unidirectional component of flow velocity
γ' Submerged weight per unit volume of sediment
θ Angle between unidirectional- and oscillatory-flow components
μ Fluid viscosity
μ_{10} Fluid viscosity standardized to 10°C water temperature
μ_r Ratio of two fluid viscosities
ρ Fluid density
ρ_r Ratio of two fluid densities
ρ_s Sediment density
σ Standard deviation of sediment size distribution
τ_o Boundary shear stress
τ_{o10} Boundary shear stress standardized to 10°C water temperature
τ_o° Dimensionless boundary shear stress.